




# On The Potential Use of Copper-Modified Geopolymer Incorporating Lead-Smelter Slag for Thermal Energy Storage

Nghia P. Tran<sup>1,2</sup> , Tuan N. Nguyen<sup>2</sup> , and Tuan D. Ngo<sup>1,2</sup> 

Building 4.0 CRC, Caulfield East, VIC 3145, Australia

<sup>2</sup> Department of Infrastructure Engineering, The University of Melbourne, VIC 3010, Australia

**Abstract.** Thermal energy storage (TES) system has been widely employed in concentrated solar power (CSP) plants to ensure the system efficiency. With excellent thermal characteristics, electrolytic copper powder (ECP), graphene oxide (GO) and lead-smelter slag (LSS) aggregate – a mining waste material, have been utilised in this study, aiming to fabricate metallurgical geopolymer material as a storage medium in the TES system. This paper investigated the effect of ECP contents (0, 5%, 10%, 15%, 20%) on the strength, specific heat, thermal conductivity and thermal stability of GO-engineered geopolymer mixes incorporating LSS aggregate. With 10% ECP inclusion, the flow rate and compressive strength improved significantly. Increasing ECP content improved the thermal conductivity but reduce specific heat of geopolymers. The results revealed that ECP was a promising component to be incorporated into geopolymer to enhance its physio-mechanical characteristics and thermal stability. The combination of ECP, GO and LSS to produce geopolymer materials for TES system can provide an eco-friendly solution to the CSP plants and the industry waste recovery.

**Keywords:** Alkali-Activated Materials, Copper, Lead-Smelter Slag, Thermal Energy Storage

## 1. Introduction

According to the statistics of BloombergNEF, the global energy storage deployment is forecasted to soar from a modest 9 gigawatts (GW) in 2018 to 1,095 GW by 2040 – an estimate of 122-fold boom within the next two decades (**Figure 1**) [1]. In the near term, renewables-plus-storage is more likely to be a critical enabler for the ‘net zero’ transition, which marks a new epoch of dispatchable renewables [2]. Various sort of storage technologies (not be limited to energy) has been evolving and put into practice, including carbon capture, pumped hydro, hydrogen, thermal, electrochemical, mechanical, electrical, and bioenergy storage. Together with other advanced technologies, thermal energy storage (TES) has increasingly become as one of the major drivers for the on-going transition to renewable energy economy. Currently, the global TES market was valued at \$US 20.8 billion as of 2022 and is projected to \$US 51.3 billion by 2030 with an estimated growth rate of 8.5% per annum [3]. The major growth of TES market size signifies the increasing demand, investment opportunities and its far-reaching influence on renewable energy economy. Therefore, the integration of TES system into concentrating solar power (CSP) plants or industrial processes has contributed to a paradigm shift and modernisation of the energy system in a bid for decarbonising the industry [4]. Among sensible TES system with storage technologies using molten salt, rock or sand – which have been commercially available in the market [5], concrete as a TES medium (CTES) has emerged as a low-cost but high-performance competitor [6]. Many cement-based CTES-

integrated systems have been deployed across the globe (including Spain, US, Germany and United Arab Emirates); namely DLR [7], Heatcrete [8] and others [9, 10]. However, utilising materials with high embodied-carbon footprint like cement concrete for TES applications is not deemed to be justifiable. It necessitates the use of alternative materials with more sustainable such as waste materials [11-15], which gain more attraction due to environmental benefits [16].

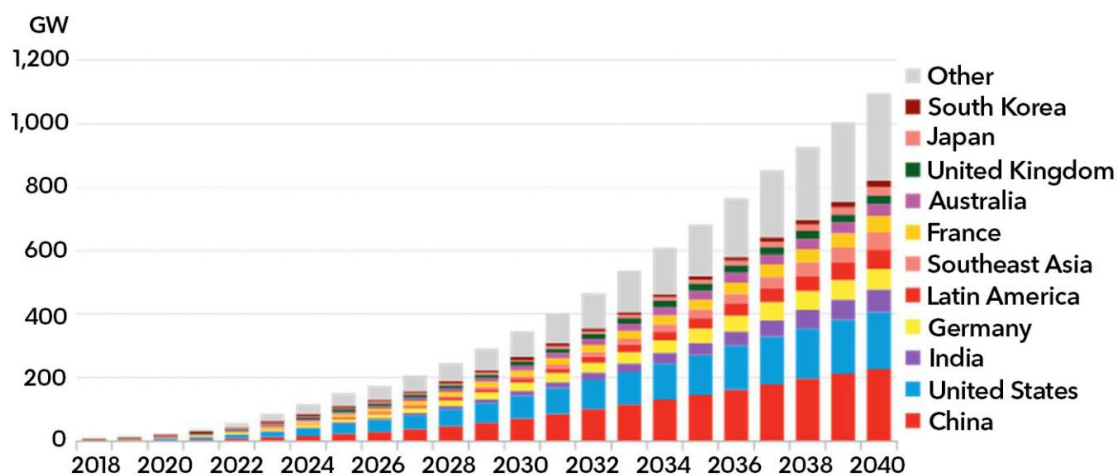


**Figure 1.** Global cumulative energy storage installations, according to statistics from BloombergNEF (BNEF).

Fly ash (FA) and ground granulated-blast furnace slag (GGBS) are industrial by-products with aluminosilicate-rich components, which offer an eco-friendly value when used in fabricating geopolymers for TES applications. The N-A-S-H and C-(A)-S-H gel structures show good thermal stability and metal cation encapsulation, implying a high compatibility with metallic inclusion. Like other metallic materials, electrolytic copper powder (ECP) with high thermal conductivity ( $\sim 400$  W/mK) is considered as a potential component in fabricating geopolymer materials for TES applications. Also, graphene nanomaterials possessing extremely high conductivity (up to 4000 W/mK) can contribute to both strengthening geopolymer structure and improving conductivity of materials for CTES system [17]. In addition, the utilisation of these metallurgical waste with either ferrous or non-ferrous components has been demonstrated their potential for serving as sensible heat storage materials in medium-high temperature TES system [18-23]. The lead-smelter slag (LSS), which is an abundant mining waste ended up in landfills and reportedly amounts to 5.5 million tons in 2016 (approx. 50% of global lead production) [24], can be utilised in augmenting thermal performance of CTES, while concurrently mitigating associated environmental impacts.

There are hardly any studies on the combined use of ECP, GO and LSS for the enhanced thermal properties of geopolymer. In the first time, this study aims to investigate the effects of ECP on thermo-mechanical performance of geopolymer materials incorporating GO and LSS for TES system. Thereupon, different contents of ECP within 0–20% with 5% interval were used for this investigation. Half of geopolymer mixes were exposed to 450°C with 5-time heat cycles, meanwhile the rest were cured at ambient condition as reference samples. Their fundamental properties including flowability, compressive strength, thermal conductivity, specific heat, and derivative thermogravimetry (DTG) were characterised to gain an understanding on the effect of ECP on the thermal performance and stability of geopolymer at elevated temperature. The outcome of this study would provide a new mix design of waste-based geopolymer materials modified by ECP with enhanced thermo-mechanical properties for high-temperature TES applications.

## 2. Experimental Methodology

### 2.1 Sample Preparation

FA (53% SiO<sub>2</sub>, 28% Al<sub>2</sub>O<sub>3</sub>, 8% Fe<sub>2</sub>O<sub>3</sub>, 7% CaO) and GGBFS (31% SiO<sub>2</sub>, 12% Al<sub>2</sub>O<sub>3</sub>, 44% CaO) were used as the aluminosilicate precursor to synthesise geopolymer specimens. The FA and GGBFS showed a specific gravity of 2.4 g/cm<sup>3</sup> and 3 g/cm<sup>3</sup>, respectively. The ECP (99.7% Cu) had a dendritic particle shape, a mean particle size of 40 μm and a specific gravity of 3.4 g/cm<sup>3</sup>. The LSS fine aggregate exhibited a specific gravity of 3.3 g/cm<sup>3</sup> and fineness modulus of 2.51. The sodium metasilicate (SMS) used in this study had a molar SiO<sub>2</sub>/Na<sub>2</sub>O of 0.9 and specific gravity of 1.2 g/cm<sup>3</sup>. The GO in suspension form with a concentration of 2.5 wt% was utilised for enhancing the thermal and mechanical performance of geopolymers. The superplasticiser (SP) was used at 1% of the total weight of precursors to improve the dispersion of particles. Overall, there were five mix designs with five different contents of ECP, ranging from 0, 5%, 10%, 15% to 20%, as labelled in **Table 1**. In all mixes, ratios of activator-to-precursor, water-to-binder and aggregate-to-binder were kept constant at 0.1, 0.4, and 2.5, respectively.

**Table 1.** Mix design of geopolymer samples (kg/m<sup>3</sup>).

Mix ID	FA	GGBFS	ECP	SMS	GO	LSS	Water	SP
ECP-0	315	315	0	63	0.6	1575	221	6
ECP-5	283	315	32	63	0.6	1575	221	6
ECP-10	252	315	63	63	0.6	1575	221	6
ECP-15	220	315	94	63	0.6	1575	221	6
ECP-20	188	315	126	63	0.6	1575	221	6

To prepare geopolymer mortars, dry solid components comprising FA, GGBFS, SMS, ECP and LSS were pre-mixed at slow speed for 2.5 minutes. The aqueous solution of water, GO suspension and SP were prepared and sonicated for 20 minutes using the sonicator Q500. Afterwards, this aqueous solution was slowly added to the dry mix and the mixing was proceeded with further 10 minutes. In between, the high-speed mixing was operated for 1 minute at 4 and 9 minutes. Subsequently, the homogeneous slurry was poured into the 50 × 50 × 50 mm<sup>3</sup> cube teflon moulds, and compacted with a support of vibrating table for 1 minute to remove entrapped air voids. The surface of specimens was then covered by plastic sheets to avert shrinkage and cracking, as followed to other studies [25, 26]. After a-day storage under a room condition (T = 23 ± 2°C, RH = 50 ± 2%), some specimens were demoulded and kept inside the plastic bag; meanwhile, other samples being subjected to heat cycles were placed inside furnace at 14 days and then kept in ambient condition until the test date. The density of these specimens was observed to vary in between 2484 and 2495 kg/m<sup>3</sup>.

### 2.2 Test Methods

The Tetlow furnace was employed for operating heat cycles. Besides reference specimens cured at ambient temperature, other geopolymer samples were subjected to 5-time heat cycles at 450°C. A heating rate was set up at 10°C/min. When the furnace reached to the targeted temperature, it was hold for 2 hours for ensuring the uniform distribution of heat throughout the samples before cooling down. The heating-cooling process was repeated 5 times, as illustrated in **Figure 2** below. For the compression test, it was conducted by Technotest machine in accordance with ASTM C109/C109M-20b. Four standard samples from each mix design were examined to obtain their data point corresponding to each test, then the mean value and standard deviation of samples were calculated accordingly. The derivative thermogravimetric (DTG) was conducted using a Perkin Elmer Simultaneous Thermal Analyzer STA 8000 with a support of Pyris™ Software. The instrument was set up at a temperature range of 30 – 500°C and a heating rate of 10°C/min. The Hot Disk TPS2500 with a planar Kapton sensor and a Cp

cell, was employed to measure the thermal conductivity and specific heat of geopolymers with three separate testing times to estimate the mean and standard deviation.

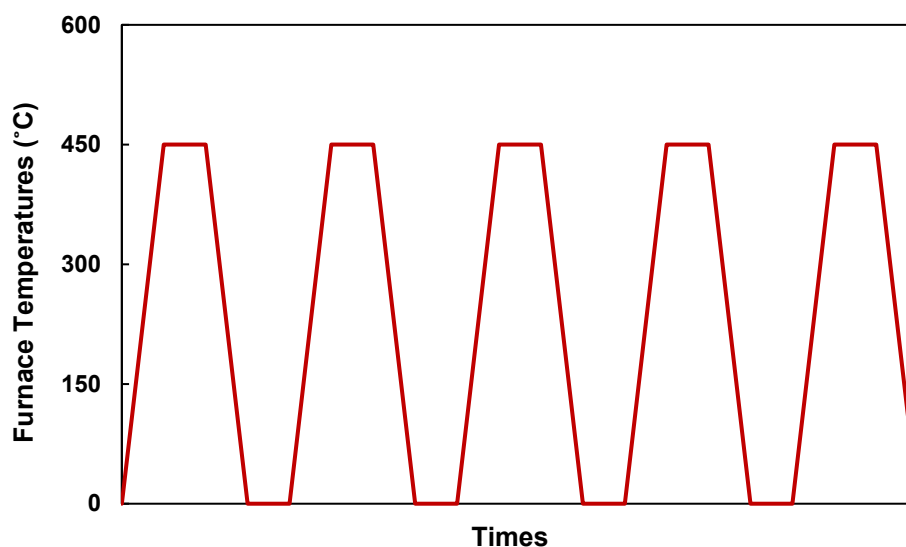


Figure 2. A diagram of heating-cooling cycles

### 3. Results and Discussion

#### 3.1 Flowability and Strength

The flowability of geopolymer mixtures is exhibited in **Figure 3**. Interestingly, there was an increase in flowability when incorporating ECP in geopolymer mortars. With the use of 5% and 10% of ECP, the flow rate increased by 5% and 8% respectively. The flowability of geopolymer mixtures reached the highest value at 38%, corresponding to 10% ECP inclusion. When the ECP content was over 10% (i.e., 15% and 20%), its positive effect on flowability was lessened, but was still higher than the control sample without ECP. The increase in flow rate with the presence of ECP could be mainly attributed to the ionic interaction of metallic ECP in the fresh mixture. Fine ECP particles with a repelling net charge were able to diminish the attractive interparticulate forces, thereby reducing viscosity and improving the flowability of geopolymer.

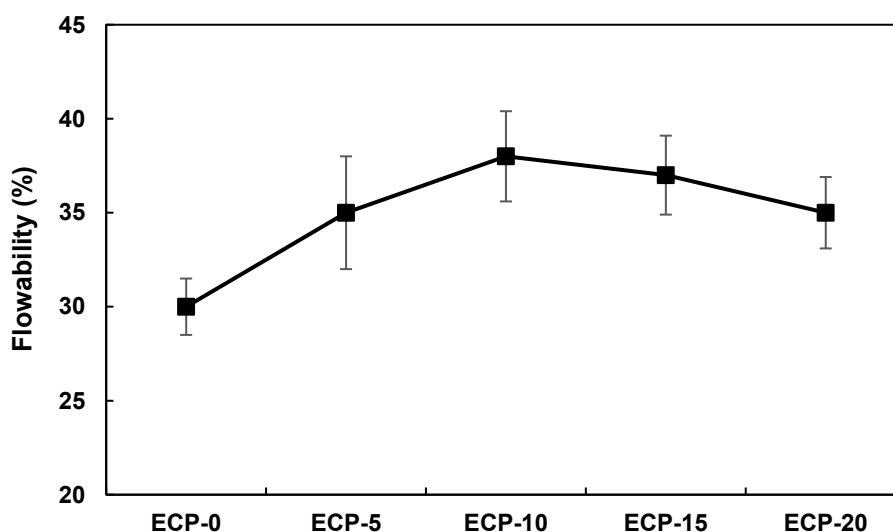
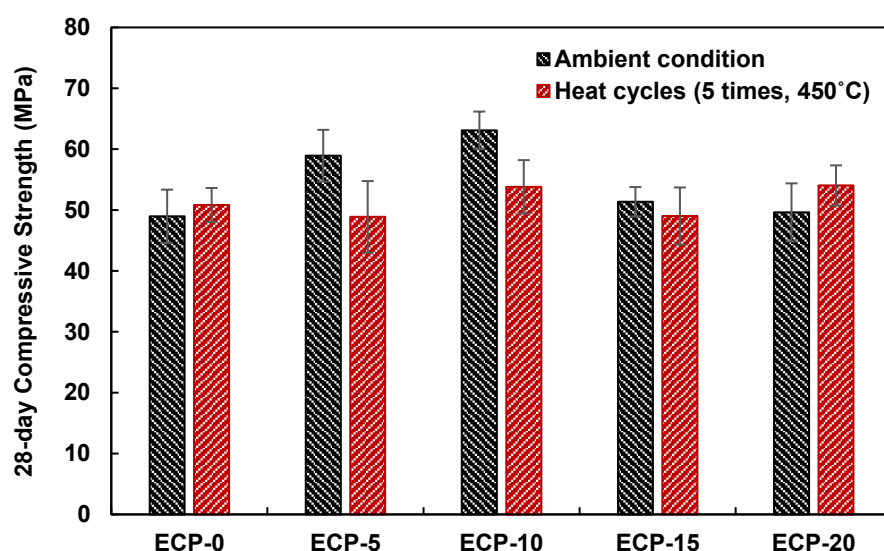


Figure 3. Flowability of fresh geopolymer mixtures with different ECP contents.

According to the result data presented in **Figure 4**, the incorporation of ECP enhanced 28-day compressive strength of geopolymer, especially with the use of 5% and 10% ECP. The positive effect of ECP on strength improvement was deemed to be higher for geopolymer samples being cured at ambient condition than those exposed to heat cycles. The ECP-10 with 10% of ECP inclusion achieved the highest 28-day strength at 63 MPa (ambient curing) and 53.8 MPa (5-time heat cycles), which were approx. 29% and 6% respectively higher than the reference sample for a similar curing method. When increasing the ECP content to 15% and 20%, the compressive strength did not improve much and had almost equivalent strength of control samples without ECP, considering samples being cured under both ambient and high heat temperature. Notably, all strength of geopolymer specimens with and without ECP, which were subjected to 5-time heating-cooling cycles at 450°C, did not show much difference and varied around 50 MPa. The presence of metallic ECP might facilitate the formation of thermally-stable phases and modified the arrangement of geopolymer chain that minimised the cracking and strength degradation of geopolymer when exposing to high temperatures and heat cycles.



**Figure 4.** 28-day compressive strength of specimens after exposing to ambient temperature and 5-time heat cycles up to 450°C.

### 3.2 Thermal Conductivity and Specific Heat

Increasing inclusion of ECP enhanced thermal conductivity but reduced specific heat of geopolymers, as observed in **Figure 5**. Thermal conductivity of geopolymer increased from 1.05 to 1.25 W/mK (approx. 5 – 19%) corresponding to the addition of 5 – 20% ECP. The improvement in thermal conductivity of the geopolymer samples could be attributed to an increase in ion concentration as well as ionic mobility in pore solution for facilitating heat transfer. After being subjected to 5-time heat cycles, thermal conductivity of all geopolymer samples was decreased by 9 – 14% as a result of water loss. On the other hand, the specific heat exhibited an opposite tendency to the thermal conductivity characteristic. It was understandable that specific heat of material was inversely proportional to its density. Higher ECP content could increase the density of geopolymer samples and thus its specific heat capacity tended to reduce. At both ambient and heat condition, their specific heat varied within 1000 – 1400 J/kg.K with the inclusion of ECP at 5 – 20%. The specific heat values of geopolymer samples being subjected to heat cycles were higher than those of samples cured at ambient temperature. Notably, The ECP-10 sample appeared to attain an equilibrium point between its thermal conductivity and specific heat properties.

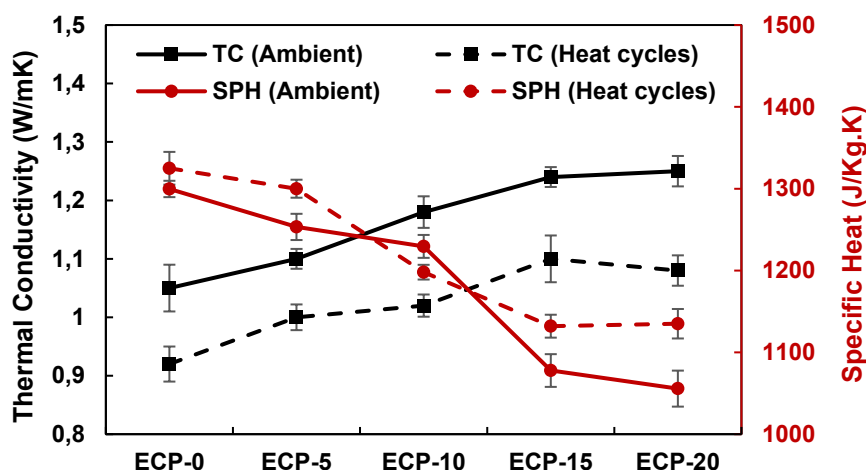


Figure 5. Thermal conductivity and specific heat of geopolymer samples.

### 3.3 Derivative Thermogravimetry (DTG)

High temperature stability of geopolymers had been improved by the incorporation of ECP, as reflected by DTG curves in **Figure 6**. Increasing ECP content from 5%, 10% to 15% resulted in a lower mass loss of geopolymer at elevated temperatures. Also, there was a threshold, where a sufficient amount of ECP could establish ionic bonds into geopolymer chain, thereby significantly contributing to the thermal stability of geopolymer matrix. Indeed, the ECP-15 samples showed a total mass loss by 9%, compared to the control ECP-0 with a mass loss of 11% after being exposed to 450°C. When exceeding the threshold of 15% ECP, a higher dose of ECP was less likely to be stable at elevated temperatures. Apparently, ECP-20 sample had higher mass loss than the ECP-15 sample throughout the duration of heat exposure. Theoretically, metal ions and its reactivity had a stable resistivity at high temperature. However, the use of high dose of ECP as the FA replacement might also trigger a reduction in N-A-S-H gel formation, which was more thermally stable than C-A-S-H gels.

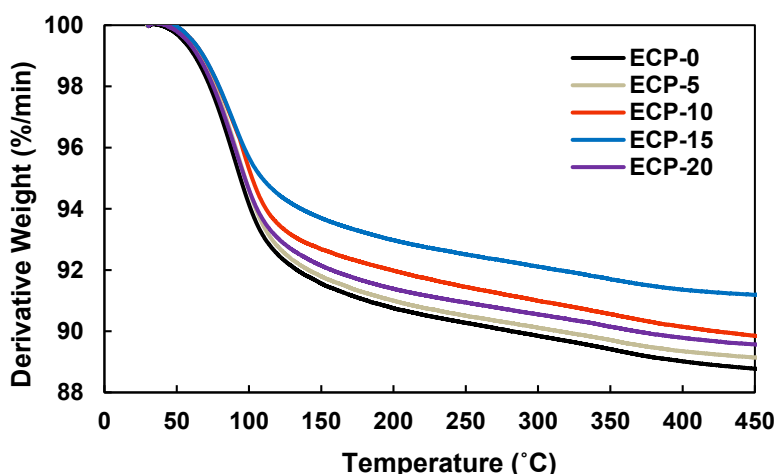


Figure 6. DTG curve of ECP-modified geopolymer samples.

## 4. Conclusions

The effect of ECP contents (i.e., 5, 10, 15, 20%) on thermo-mechanical performance of GO-engineered geopolymer incorporating LSS aggregate was investigated in this study. There is a threshold of ECP content ( $\leq 15\%$ ) to be effectively used for producing geopolymer with a

significant enhancement on flowability, strength and thermal stability. The addition of ECP improves the thermal conductivity but reduce specific heat of geopolymers when exposing to both heat cycles and ambient conditions. Overall, this result demonstrates the potential use of ECP on enhancing physio-thermo-mechanical properties of geopolymer materials for high-temperature TES applications. These findings also open a pathway for future research to explore the microstructure and chemical kinetics of ECP-modified waste-based geopolymer.

## Data availability statement

All data, models, and code generated or used during the study appear in the published article.

## Author contributions

**Nghia P. Tran:** Conceptualization, Methodology, Software, Data curation, Formal analysis, Investigation, Visualization, Validation, Writing – original draft. **Tuan N. Nguyen:** Methodology, Supervision, Writing – review & editing, Project administration. **Tuan D. Ngo:** Methodology, Supervision, Writing – review & editing, Funding acquisition.

## Competing interests

The authors declare that they have no competing interests.

## Acknowledgement

The first author gratefully acknowledges the financial support from the Building 4.0 CRC and Melbourne Research Scholarship in order to conduct this research.

## References

1. Henze, V. Energy Storage Investments Boom As Battery Costs Halve in the Next Decade. 2019.
2. International Energy Agency (IEA), World Energy Outlook 2022. 2022.
3. Arbaz, M. and E. Prasad, Global Thermal Energy Storage Market - Opportunity Analysis and Industry Forecast, 2020-2030. 2022: United States.
4. Enescu, D., et al., Thermal Energy Storage for Grid Applications: Current Status and Emerging Trends. *Energies*, 2020. 13(2): p. 340.
5. Dunn, R., P. Hearps, and M. Wright, Molten-Salt Power Towers: Newly Commercial Concentrating Solar Storage. *Proceedings of the IEEE*, 2012. 100: p. 504-515.
6. Rahjoo, M., et al., Thermal Energy Storage (TES) Prototype Based on Geopolymer Concrete for High-Temperature Applications. *Materials (Basel)*, 2022. 15(20).
7. Laing, D., et al., Solid media thermal storage for parabolic trough power plants. *Solar Energy*, 2006. 80(10): p. 1283-1289.
8. Hoivik, N., et al., Long-term performance results of concrete-based modular thermal energy storage system. *Journal of Energy Storage*, 2019. 24: p. 100735.
9. Laing, D., et al., High-Temperature Solid-Media Thermal Energy Storage for Solar Thermal Power Plants. *Proceedings of the IEEE*, 2012. 100(2): p. 516-524.

10. Vigneshwaran, K., et al., Concrete based high temperature thermal energy storage system: Experimental and numerical studies. *Energy Conversion and Management*, 2019. 198: p. 111905.
11. Tran, N.P., et al., Comprehensive review on sustainable fiber reinforced concrete incorporating recycled textile waste. *Journal of Sustainable Cement-Based Materials*, 2022. 11(1): p. 28-42.
12. Tran, N.P., et al., Utilization of Recycled Fabric-Waste Fibers in Cementitious Composite. *Journal of Materials in Civil Engineering*, 2023. 35(1): p. 04022372.
13. Tran, N.P., et al., Repurposing of blended fabric waste for sustainable cement-based composite: Mechanical and microstructural performance. *Construction and Building Materials*, 2023. 362: p. 129785.
14. Tran, N.P., et al., Microstructural characterisation of cementitious composite incorporating polymeric fibre: A comprehensive review. *Construction and Building Materials*, 2022. 335: p. 127497.
15. Tran, N.P., T.N. Nguyen, and T.D. Ngo, The role of organic polymer modifiers in cementitious systems towards durable and resilient infrastructures: A systematic review. *Construction and Building Materials*, 2022. 360: p. 129562.
16. Tran, N.P., et al., Strategic progress in foam stabilisation towards high-performance foam concrete for building sustainability: A state-of-the-art review. *Journal of Cleaner Production*, 2022. 375: p. 133939.
17. Tran, N.P., et al., High-temperature stability of ambient-cured one-part alkali-activated materials incorporating graphene nanoplatelets for thermal energy storage. *Developments in the Built Environment*, 2024. 18: p. 100447.
18. Ortega-Fernández, I., et al., Experimental validation of steel slag as thermal energy storage material in a 400 kWh prototype. *AIP Conference Proceedings*, 2019. 2126(1).
19. Wang, J. and Y. Huang, Exploration of steel slag for thermal energy storage and enhancement by Na<sub>2</sub>CO<sub>3</sub> modification. *Journal of Cleaner Production*, 2023. 395: p. 136289.
20. Ortega-Fernández, I., et al., Thermophysical characterization of a by-product from the steel industry to be used as a sustainable and low-cost thermal energy storage material. *Energy*, 2015. 89: p. 601-609.
21. Boquera, L., et al., Thermo-mechanical stability of concrete containing steel slag as aggregate after high temperature thermal cycles. *Solar Energy*, 2022. 239: p. 59-73.
22. Vu Hong Son, P., et al., Steel slag aggregate low-cement concrete: Engineering performance, microstructure and sustainability. *Construction and Building Materials*, 2024. 436: p. 136827.
23. Krüger, M., J. Haunstetter, and S. Zunft, Slag as an inventory material for heat storage in a concentrated solar tower power plant: Final project results of experimental studies on design and performance of the thermal energy storage. *AIP Conference Proceedings*, 2020. 2303(1).
24. Pan, D.a., et al., A review on lead slag generation, characteristics, and utilization. *Resources, Conservation and Recycling*, 2019. 146: p. 140-155.
25. Tran, N.P., et al., A critical review on drying shrinkage mitigation strategies in cement-based materials. *Journal of Building Engineering*, 2021. 38: p. 102210.
26. Tran, N.P., et al., Upcycled Polypropylene and Polytrimethylene Terephthalate Carpet Waste in Reinforcing Cementitious Composites. *ACI Materials Journal*, 2022. 119(4).